UNMANNED AERIAL VEHICLES FOR RANGELAND MAPPING AND MONITORING: A COMPARISON OF TWO SYSTEMS

Andrea S. Laliberte, Remote Sensing Scientist
Albert Rango, Research Hydrologist
Jeff Herrick, Rangeland Scientist
USDA-Agricultural Research Service, Jornada Experimental Range
New Mexico State University, Las Cruces, NM 88003
alaliber@nmsu.edu, alrango@nmsu.edu, jherrick@nmsu.edu

ABSTRACT

Aerial photography from unmanned aerial vehicles (UAVs) bridges the gap between ground-based observations and remotely sensed imagery from aerial and satellite platforms. UAVs can be deployed quickly and repeatedly, are less costly and safer than piloted aircraft, and can obtain very high-resolution imagery. At the Jornada Experimental Range in New Mexico, ongoing research is aimed at determining the utility of UAVs for rangeland mapping, assessment and monitoring. Digital images of arid rangelands were acquired with two UAVs that differed in size/weight, payload capacity, flight duration, GPS guidance capability and cost. The first system was a modified model airplane equipped with GPS and able to fly along preloaded waypoints and acquire images with a digital camera. The second UAV was a BAT 3 (MLB Systems) with fully autonomous flight capability and equipped with color video and digital cameras. Both units provide a data file containing GPS and elevation for each image, but the

At the USDA Agricultural Research Service's Jornada Experimental Range (JER) in southern New Mexico, ongoing research is aimed at determining the utility of UAVs for rangeland mapping and monitoring, and developing a workflow consisting of acquisition, orthorectification, mosaicking, and classification of UAV imagery. An additional goal is to relate remotely sensed information from the imagery to ground-based rangeland monitoring measurements that have been developed and tested at the JER (Herrick et al., 2005; 2006a). We are currently pursuing two parallel tracks of investigation for UAV applications. The first is the use of a modified model airplane designed to minimize costs and maximize simplicity for monitoring purposes. The second consists of a technologically more advanced UAV capable of carrying a variety of sensors for research purposes. The objective of this paper is to describe and compare details of both unmanned systems, to present results of test flights conducted at the JER, and to assess the results of image acquisition, rectification, mosaicking and classification.

UAV PLATFORMS

The modified model airplane used in the test flights (Figure 1) has a payload capacity of approximately 1 kg and a flight duration of approximately 30 minutes, limited by the 0.4-liter gas tank. It is equipped with a Sony DSC P-200 7 megapixel digital camera, a Garmin eTrex GPS unit, an autopilot system, and a flight stabilizer. The camera, batteries, GPS unit, and control circuits are located in the plane's body and a cargo pod strapped underneath (Figure 2). The flight line's endpoint coordinates are uploaded to the GPS unit, and after the plane is in the air, it acquires the initial waypoint and begins its autonomous flight. After the first waypoint, the camera is triggered automatically every two seconds until the end of the flight line is reached. The plane is then landed manually. For each image, a GPS coordinate, elevation and time stamp are recorded in a text file.

Figure 1. Modified model airplane with yellow cargo pod holding camera, controller and data recorder.

Figure 2. Interior of the plane's body (left) and cargo pod (right) holding GPS unit (a), autopilot (b), flight stabilizer (c), altitude control (d), shutter servo (e), data recorder (f), camera controller (g), GPS data cable (h), Sony P-200 digital camera (i), and power supply (j).

The technologically more advanced UAV we used is a MLB BAT 3 UAV (MLB Company, 2006)[1]. The BAT system consists of a fully autonomous GPS-guided UAV, a catapult launcher, ground station with mission planning and flight software, and telemetry system (Figure 3). Once launched off the catapult, the BAT acquires the first waypoint, flies the programmed flight lines and acquires images at 60% forward lap and 30% side lap for future mosaic production. The moving map display on the ground station shows the aircraft's location and other parameters, such as speed, altitude, and fuel level in real time while the UAV is within 10 km of the ground station. Waypoints can be changed and uploaded in real time to the aircraft. The UAV currently carries two sensors: a color video camera with optical zoom capable in-flight and live video downlink to the ground station, and a Canon SD

[1] Mention of trade names or commercial products in this publication is solely for the purpose of providing specific information and does not imply recommendation or endorsement by the US Department of Agriculture.

550 7 megapixel digital camera. In the future, we plan to update sensors as miniaturized versions become available. The BAT lands autonomously in a 100 m x 50 m area. The onboard computer records a timestamp, GPS location, elevation, pitch, roll, and heading for each acquired image. In addition, airspeed, altitude, fuel level, rpm, wind speed and wind direction are recorded every second and saved to text and graphics files that are downloaded after landing. For comparison purposes, details of both UAVs are displayed in Table 1.

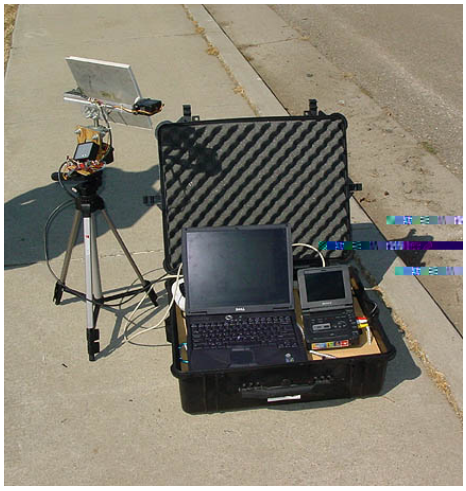

Figure 3. BAT 3 UAV on catapult launcher ready for takeoff (left). Ground station with laptop and video deck used for live video downlink, and telemetry antenna (right).

Table 1. Details of the two UAVs used in this study

	Modified Model Airplane	**BAT 3 UAV**
Size/Weight	1.8 m wingspan/5.2 kg	1.8 m wingspan/10 kg
Payload capacity	1.1 kg	1.2 kg with current sensor, 2.3 kg without
Flight duration/max. altitude	30 min./1000 m	2-6 hours/3000 m
Sensors	Sony DSC P-200 7 MP camera	Color video w. live downlink, Canon SD 550 7 MP camera
Takeoff and landing	Radio controlled takeoff and landing	Catapult launch, autonomous landing
Guidance system	Flies along preloaded waypoints	Fully autonomous GPS guided by flight computer
Data recorded	X,Y,Z	X,Y,Z, roll, pitch, heading
Cost	~ $2,500	~ $52,000

IMAGE ACQUISITION

Images were acquired with the modified model airplane in June 2006 and with the BAT in October 2006. The Sony P-200 camera and the Canon SD 550 both have the same sensor size (7.18 mm x 5.32 mm) and resolution (3072 x 2304 pixels) with a field of view of 53.1 degrees. Therefore, the resulting image footprint on the ground was the same from both UAVs, measuring 152 m x 114 m, and the pixel resolution was 5 cm (example is based on a flying height of 150 m above ground).

With the modified model airplane, we completed two successful GPS-guided flights, but on the third flight, the aircraft was not able to acquire the first waypoint and we proceeded with manual radio-controlled flight. This problem was later traced to a malfunction on the autopilot board. With manual control, it is difficult to maintain the plane on a straight flight line and to fly at a predetermined altitude. With the autopilot system, the GPS-controlled altitude hold circuit is designed to keep the plane within approximately 10 m of the desired altitude. However, even with the autopilot system, the plane was affected by wind and thermals, which are common in the desert environment in the summer. The flight line in Figure 4 was flown with the autopilot engaged, and it was planned as

a straight line between the end points. As can be seen, the aircraft was affected by wind from the east. The graph shows the variation in elevation along the same flight line. At 180 seconds into the flight, the aircraft gained 37 m in less than 1 minute, and then dropped back down in elevation. This sudden increase in altitude was due to thermals that lifted the light plane up. Over the course of the 6-minute flight time, the difference between minimum and maximum elevation was 40 m.

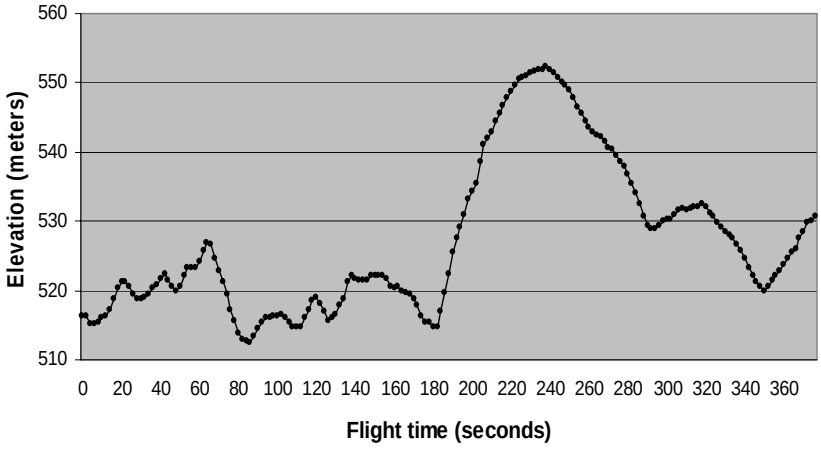

Figure 4. Center locations of 189 images acquired with the modified model airplane along one flight line (left), and associated elevation changes (right). Images were acquired every 2 seconds. Flight line points are overlayed on a pansharpened QuickBird image.

Compared to the modified model airplane, the BAT has more stability due to its larger weight and more sophisticated autopilot system. Over the course of a 19-minute flight, the difference between minimum and maximum elevation was only 15 m (Figure 5). During this flight, the wind was blowing from a southwesterly direction, and the footprints show that the BAT crabbed into the wind as it flew from north to south. However, the UAV maintained a straight north-south flight line, and the distances between image center locations remained approximately the same, because we were able to control the flight speed based on wind speed and direction.

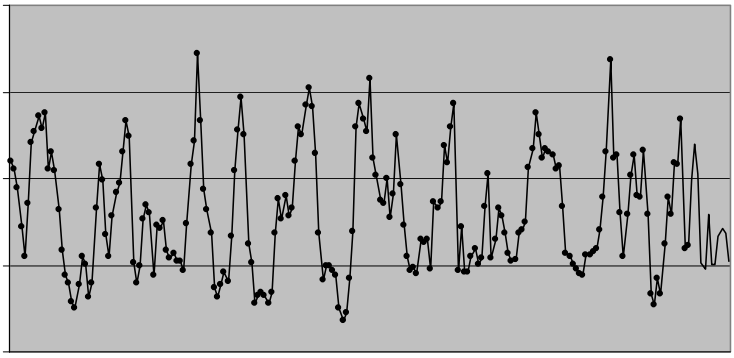

The BAT UAV proved to be very reliable for image acquisition. Over a 3-day period, we acquired 5145 images in 13 hours flight time, limiting the flying time between 9:30 am and 2:30 pm to eliminate shadows. We acquired imagery over approximately 90 sq km at 5 cm pixel resolution. We launched and landed the BAT from a central airstrip at the Jornada Experimental Range (Figure 6), and flew six missions, denoted by the different colors. Images were acquired as far away as 14 km from the airstrip, and the longest mission lasted 1½ hours. We found that our limitation was the capacity of the four-gigabyte memory card in the camera rather than the BAT's endurance ability. At approximately four megabytes per image, we could acquire about 1000 images before we had to land to download the camera's memory card.

We were able to fly under varying weather conditions ranging from clear and calm to rainy with winds up to 15 km/hour. If the wind was strong, we increased the UAV's speed flying into the wind and reduced it when flying with the wind, so that the image overlap would remain constant. Throughout the entire mission, we did not experience any technical malfunctions.

Figure 6. Coverage of BAT UAV imagery acquired in 13 hours flight time over a 3-day period at the Jornada Experimental Range in southern New Mexico. The different colors denote six different missions.

IMAGE PROCESSING

Raw Imagery

The image quality from both cameras was excellent (Figure 7) and comparable for both platforms, although some images taken with the modified model airplane displayed slight blurriness due to vibration effects. The difference between the two systems lies in the associated image information. With the modified model airplane, a GPS coordinate and elevation are recorded for each image, while with the BAT, in addition to this information, the roll, pitch, and heading of the platform are also known. Knowing six, rather than three parameters for each image

Figure 7. Images acquired from the modified model airplane (left) and from the BAT UAV (right) from 150 m above ground. Image extent is approximately 152 m x 114 m.

can simplify aerial triangulation and orthorectification of the imagery. Since the modified model airplane was flown in June and the BAT in October, imagery from the model airplane was processed first. Lessons learned were then applied to the processing of the BAT imagery.

Images from Modified Model Airplane

We selected eight images acquired with the modified model airplane, chosen for their excellent image quality, little or no effects of vibration, near nadir acquisition, and location over heterogeneous rangeland vegetation. The images were orthorectified using Leica Photogrammetric Suite 9.0 (LPS) (Leica Geosystems Geospatial Imaging, LLC). Ground coordinates of 32 ground control points (GCPs) were acquired with a Trimble Pro XR GPS unit and differentially corrected. During image processing, we noticed that the image center coordinates recorded during flight did not coincide with the visually estimated image center coordinates, as estimated from a QuickBird satellite image. For the eight images, the average difference between GPS-recorded and visually estimated image centers was 31.02 m +/- 6.9 m. At the small footprint size of those images, this discrepancy represents 16% of image width and 22% of image height. We found that using the GPS-acquired image center coordinate represented too large of an error for processing in the LPS software and resulted in an inability of the software to acquire automatic tie points or solve the aero triangulation. For that reason, we visually estimated the image center coordinates by comparison with a QuickBird image.

The error in the center coordinate can have several sources. One source is GPS error, and we compared the Garmin eTrex unit with a Trimble XT® GPS in a static test using 1469 points. The results showed that the error ranged from 4 m for 50% of the points to 13 m for 98% of the points. Other sources of error include pitch and roll angles, and the influence of sudden wind gusts.

We had difficulties in processing the entire strip of eight images because of problems with automatic tie point selection, aero triangulation, and orthorectification. Using only two images rather than eight resulted in a reduced RMS error (1.4 pixels for two images compared to 16.9 pixels for eight images). We concluded that there was too much image distortion in each individual image to process the entire strip with small enough RMS error. However, by processing only two images at a time, a satisfactory mosaic of the orthorectified images was produced (Figure 8).

Image classification was performed using Definiens Professional 5.0. Using an object-based image classification procedure is more suitable than pixel-based classification for high and very high resolution imagery (Hodgson et al., 2003; Yu et al., 2006; Laliberte et al., 2007a; 2007b). We were able to map snakeweed, a small shrub with an approximate canopy diameter of 30-50 cm, and we could differentiate two types of bare soil as well as dense and sparse tobosa grass cover. The overall classification accuracy was 96% with a Kappa Index of Agreement of 0.94. Producers and users accuracy was in the mid to high 90% range.

Figure 8. Orthorectified mosaic of imagery acquired with modified model airplane (left), object-based classification (middle), and enlarged portions of both images within the red rectangle (right).

Images from BAT UAV

Based on the difficulties experienced during aero triangulation and orthorectification of the above imagery, we decided to perform a camera calibration on the imagery acquired with the BAT UAV. Camera calibration is a process that measures the radial lens distortion, principal point offset, and actual focal length of a camera (Fryer, 1996). Using camera calibration parameters increases the accuracy of the orthorectified imagery and image-derived digital elevation models (Clarke and Fryer, 1998; Remondino and Fraser, 2006).

We used PhotoModeler Pro 5 (Eos Systems Inc., 2006) for camera calibration. The calibration procedure consists of taking a minimum of eight photos of a calibration grid with the same camera settings as those used during aerial photo acquisition. The modeled parameters are input into LPS, and are used during the aero triangulation process. The radial distortion curve derived from the calculated coefficients shows the considerable distortion near the edge of the images, which explains the difficulties experienced during photogrammetric processing without those parameters.

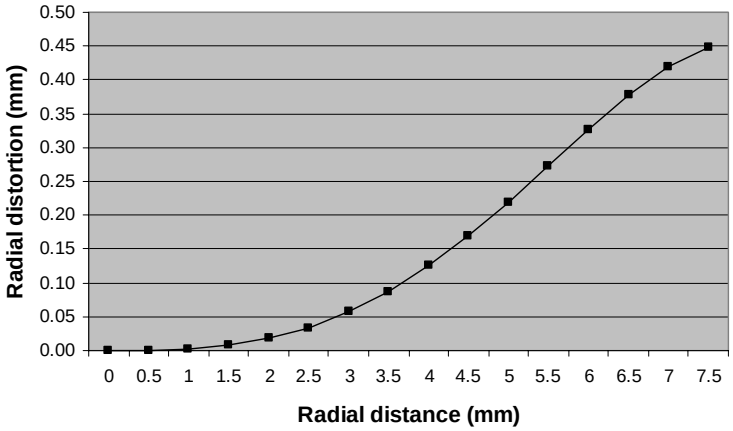

Fig. 9. Radial distortion curve for the Canon SD 550 camera used in the BAT UAV.

We chose eight images depicting a set of constructed shallow dikes designed to retain water and promote vegetation growth (Rango et al., 2006a). The images were processed in LPS in the same manner as for the modified model airplane images, with the exception that the exterior orientation information included roll, pitch, and heading in addition to the X- and Y-coordinates and elevation. Similar to the images from the modified model airplane, the BAT image center coordinates were on average 30 m off the estimated image centers, and this resulted in numerous wrong automatic tie points and an inability of LPS to solve the aero triangulation. For that reason, we proceeded without using any of the images' exterior orientation information, selected 14 GCPs from a digital orthoquad, and subsequently LPS was able to generate sufficient automatic tie points (n=233) which were all correct. The RMS error from the aero triangulation was 0.3318 pixels (ground X: 0.6056; ground Y: 0.2614; ground Z: 0.1170).

Those results show that incorporating camera calibration information greatly reduces the RMS error from aero triangulation. Without the camera calibration parameters and no exterior information, LPS was unable to generate sufficient tie points or aero triangulate. That was the reason that we had originally estimated the image centers for the modified model airplane images. Even though the center point coordinates from the BAT or the modified model airplane are useful for locating the general area where imagery was acquired, this study shows that the accuracy of the exterior orientation parameters is not sufficient at this point for inclusion into photogrammetric processing. A higher parameter accuracy would also be needed to simplify the processing and reduce the number of ground control points needed, which always represents a time consuming step in image processing. For the BAT imagery, we used GCPs derived from a DOQ, which at 1 m resolution is quite coarse compared to the BAT imagery. If differentially corrected GPS coordinates were to be used, an even higher accuracy would be expected.

The mosaic from the BAT images showed better edge matching than the mosaic from the modified model airplane images, and the BAT image mosaic displayed perfect overlay with the DOQ. We also created a digital elevation model (DEM) from the 8 images (Fig. 10). There was lack of overlap between the 2nd and 3rd image, where no elevation values could be generated. The image orientation shows that the UAV was off-course from the rest of the image strip. The pitch value was 12 degrees for the 2nd image, and it appears that wind had affected the UAV. Although the DEM accuracy has to be assessed in more detail, lower elevations in ditches and higher elevations in vegetated areas are depicted correctly. Several artifacts are probably due to the lack of sufficient ground control.

Fig. 10. Orthorectified mosaic of imagery acquired with BAT UAV (left), and image-derived DEM.

CONCLUSIONS, RECOMMENDATIONS, AND FUTURE RESEARCH

Our experiences with acquiring and processing sub-decimeter resolution imagery from UAVs demonstrate that this approach is feasible and effective for rangeland mapping and monitoring. The UAV imagery offers opportunities to map vegetation species and quantify soil and vegetation patterns in ways not possible with aerial or

considerably distorted. Removing the image distortion greatly improved aero triangulation and orthorectification results in LPS in this study, allowed for processing the entire image strip instead of two images at a time, and resulted in an RMS error of approximately 1/3 pixel size.

UAVs have the capacity to become an important tool for assessment and monitoring of rangelands and other natural resources. As the technology improves and smaller, lightweight multispectral and hyperspectral sensors become available, UAVs will become more commonplace in natural resource applications.

REFERENCES

Bestelmeyer, B. T., D.A. Trujillo, A.J. Tugel, and K.M. Havstad. (2006). A

65:235-52.
Rango, A., A.S. Laliberte, C. Steele, J.E. Herrick, B. Bestelmeyer, T. Schmugge, A. Roanhorse, and V. Jenkins. (2006b). Using unmanned aerial vehicles for rangelands: current applications and future potentials. *Environmental Practice*, 8:159-168.
Remondino, F., and C. Fraser. (2006). Digital camera calibration methods: considerations and comparisons. *ISPRS Commission V Symposium: Image Engineering and Metrology* , Sept. 25-27, Dresden, Germany, 266-272.
Tomlins, G. F., and Y. J. Lee. (1983). Remotely piloted aircraft - an inexpensive option for large-scale aerial photography in forestry applications. *Canadian Journal of Remote Sensing*, 9(2):76-85.
Yu, Q., P. Gong, N. Clinton, G. Biging, M. Kelly , and D. Schirokauer. (2006). Object-based detailed vegetation classification with airborne high spatial resolution remote sensing imagery. *Photogrammetric Engineering and Remote Sensing*, 72(7):799-811.